CHEMISTRY OF MATERIALS
Article

Chem. Mater. **2010,** *22,* 2563–2572 2563
DOI:10.1021/cm9035677

Physicochemical Properties and Catalytic Behavior of the Molecular Sieve SSZ-70

Raymond H. Archer,[†] John R. Carpenter,[†] Son-Jong Hwang,[†] Allen W. Burton,[‡] Cong-Yan Chen,[‡] Stacey I. Zones,[‡] and Mark E. Davis*,[†]

[†]*Chemical Engineering, California Institute of Technology, Pasadena California 91125, and* [‡]*Chevron Energy Technology Company, 100 Chevron Way, Richmond California 94802*

Received November 24, 2009. Revised Manuscript Received February 9, 2010

SSZ-70 is synthesized using 1,3-bis(isobutyl)imidazolium, 1,3-bis(cyclohexyl)imidazolium, and 1,3-bis(cycloheptyl)imidazolium structure directing agents (SDAs), and the solids obtained are characterized by powder X-ray diffraction (XRD), ^{29}Si magic angle spinning nuclear magnetic resonance (MAS NMR), electron microscopy, nitrogen and hydrocarbon adsorption, and thermogravimetric analyses. The physicochemical properties of SSZ-70 show that it is a new molecular sieve that has similarities to MWW-type materials. The catalytic behavior of SSZ-70 is evaluated through the use of the constraint index (CI) test. Distinct differences in the reactivity between Al-SSZ-70 and SSZ-25 (MWW) are observed and are the consequences of the structural differences between these two molecular sieves.

Introduction

SSZ-70 is a new molecular sieve with unknown structure that was originally prepared by workers at Chevron.[1] The original syntheses of SSZ-70 involved borosilicate reaction conditions using the 1,3-diisopropylimidazolium structure directing agent (SDA). The borosilicate versions of SSZ-70 are not useful as catalysts for reactions that require strong acidity. We recently completed a study employing 16 imidazolium structure directing agents (SDAs) and approximately 160 inorganic reactions to investigate the synthesis of molecular sieve SSZ-70.[2] In that work, we were able to expand the types of SSZ-70 materials that could be prepared by direct synthesis to include pure silica and aluminosilicate compositions. Initial characterizations of borosilicate SSZ-70 suggested that SSZ-70 may have structural features similar to SSZ-25/MCM-22 (MWW), although the crystal structure of SSZ-70 remains unknown (molecular sieve frameworks are denoted by three-letter codes that can be found at www.iza-structure.org/databases/). Because of the commercial importance of MWW-type molecular sieves as heterogeneous catalysts and the fact that we can now prepare direct synthesis aluminosilicate versions (as contrasted with postsynthetic conversions of the borosilicate) of SSZ-70, a more complete understanding of the physicochemical properties and catalytic behavior of aluminosilicate SSZ-70 is merited, especially catalytic reaction comparisons with other MWW zeolites.

Pure-silica fluoride reactions typically yield solids with the BEA* topology for many imidazolium SDAs at $H_2O/SiO_2 = 3.5$, while SSZ-70 typically occurs at intermediate and high H_2O/SiO_2 ratios (7.5 and 14.5, respectively). Previous studies using identical inorganic conditions showed a transition in product framework density from low to high with increasing H_2O/SiO_2 ratios.[3] One particularly common transition was BEA* to MTW with increasing water content. The SSZ-70 occurrences suggested that it should have a micropore volume between BEA* and MTW. In addition, a sharp delineation in SSZ-70 occurrence was observed between three bis(C7) substituted SDAs (1,3-bis(cycloheptyl)imidazolium, 1,3-bis(norbornyl)-imidazolium, and 1,3-bis(cyclohexylmethyl)imidazolium) and the bis(C8) SDA 1,3-bis(cyclooctyl)imidazolium.[2] These results suggested a feature may be present in SSZ-70 that could not accommodate the larger cyclooctyl ring, although caution must be exercised as kinetic factors dominate product selectivity.

Here, SSZ-70 was synthesized using 1,3-bis(isobutyl)-imidazolium (**1**), 1,3-bis(cyclohexyl)imidazolium (**2**), or 1,3-bis(cycloheptyl)imidazolium (**3**) SDAs based on results from the full synthesis study.[2] These SSZ-70 materials were investigated further, and the catalytic activity of aluminum-containing SSZ-70 (Al-SSZ-70) was compared to SSZ-25 using the constraint index test (CI test).[4]

*To whom correspondence should be addressed. Phone: (626) 395-4251. Fax: (626) 568-8743. E-mail: mdavis@cheme.caltech.edu.

(1) Zones, S. I.; Burton, A. W. Molecular Sieve SSZ-70 Composition of Matter and Synthesis Thereof. U.S. Patent 7,108,843, September 19, **2006**.
(2) Archer, R. H.; Zones, S. I.; Davis, M. E. Microporous Mesoporous Mater. In press.
(3) Camblor, M. A.; Villaescusa, L. A.; Diaz-Cabanas, M. J. *Top. Catal.* **1999**, *9*(1−2), 59–76.
(4) Frillette, V. J.; Haag, W. O.; Lago, R. M. *J. Catal.* **1981**, *67*(1), 218–222.

© 2010 American Chemical Society
Published on Web 03/04/2010

Experimental Section

Structure Directing Agent Synthesis. All reagents were purchased from commercial vendors and used as received. Liquid NMR spectra were recorded in deuterated dimethylsulfoxide (DMSO-d_6) on 300 MHz Varian Mercury spectrometers. Combustion analysis (for guest molecule C, H, and N) was performed at the Chevron Energy Technology Center (Richmond, CA) using a Carlo-Erba Combustion Elemental Analyzer. All SDAs were exchanged to the hydroxide form using Dowex Monosphere 550A UPW hydroxide resin (Supelco). The final hydroxide concentration was determined by titration with 0.01 N HCl solution to a phenolphthalein end point.

1,3-Diisobutylimidazolium Bromide (***1***). Isobutylamine (7.32 g, 100 mmol, Alfa-Aesar, 99%) in 100 mL of toluene (EMD, ACS Reagent) was placed in a room temperature water bath, and then paraformaldehyde (3.16 g, 100 mmol, Fisher, 95%) was added with strong stirring. The solution was stirred at room temperature for 30 min, and then ice was added to the water bath. Hydrobromic acid solution (16.87 g, 100 mmol, Sigma-Aldrich, 48 wt %) was diluted to 20 wt % with 23.66 g of water and then placed on ice for approximately 1 h. After the toluene solution was cooled for 1 h, another 7.32 g (100 mmol) of isobutylamine was added dropwise via an addition funnel. The cold hydrobromic acid solution was added dropwise via an addition funnel. The ice bath was removed, and the solution was allowed to warm for approximately 2 h. Subsequently, glyoxal solution (14.52 g, 100 mmol, Alfa-Aesar, 40 wt % in water) was added dropwise. The reaction was stirred at room temperature for approximately 36 h. The solution was concentrated by rotary evaporation to give a viscous yellow/orange oil. Purification was achieved by adding 125 mL of water and 20 mL of saturated $KHCO_3$ and extracting with diethyl ether (2 × 100 mL). The aqueous phase was treated with 1.55 g of activated carbon (Sigma-Aldrich) and stirred overnight at room temperature. The carbon was filtered off and washed with a small amount of water. This process was repeated three times until the filtrate was colorless to the eye. The filtrate was concentrated by rotary evaporation, and the was residue extracted with chloroform (2 × 100 mL) and then filtered. The chloroform extracts were combined, dried over $MgSO_4$, filtered, and stripped down by rotary evaporation to give a waxy residue. Further drying under high vacuum yielded 20.57 g of off-white solid (78.7 mmol, 79% yield). ^{1}H NMR (300 MHz, DMSO-d_6): 9.41, 7.88, 4.06, 2.11, 0.85. ^{13}C NMR (75 MHz, DMSO-d_6): 136.4, 122.8, 55.4, 28.7, 19.0. Analysis calculated for $C_{11}H_{21}BrN_2$: C, 50.58; H, 8.10; N, 10.72. Found: C, 50.27; H, 8.23; N, 10.61.

1,3-Bis(cyclohexyl)imidazolium Tetrafluoroborate (***2***). Cyclohexylamine (19.83 g, 200 mmol, Alfa-Aesar, 98+%) in 200 mL of toluene (EMD, ACS Reagent) was placed in a room temperature water bath, and then paraformaldehyde (6.32 g, 200 mmol, Fisher, 95%) was added with strong stirring. The solution was stirred at room temperature for 30 min, and then ice was added to the water bath. After the solution was cooled for 1 h, another 19.83 g (200 mmol) of cyclohexylamine was added dropwise via an addition funnel. Tetrafluoroboric acid (36.60 g, 200 mmol, Alfa-Aesar 48 wt % in water) was diluted to 30 wt % with water and then added dropwise via an addition funnel. The ice bath was removed, and the solution allowed to warm for 30 min. Subsequently, glyoxal solution (28.98 g, 200 mmol, Alfa-Aesar, 40 wt % in water) was added dropwise. The flask was heated at 40 °C overnight and then allowed to cool to room temperature. The solid precipitate was filtered off and washed with 150 mL of water and then 150 mL of diethyl ether and dried overnight under high vacuum. Recrystallization from 2:1 ethyl acetate/dichloromethane yielded 33.72 g of off-white solid after drying under high vacuum (105.3 mmol, 53% yield). ^{1}H NMR (300 MHz, DMSO-d_6): 9.19, 7.88, 4.24, 2.07−2.03, 1.84−1.62, 1.43−1.30, 1.24−1.15. ^{13}C NMR (75 MHz, DMSO-d_6): 133.5, 120.8, 58.8, 32.4, 24.6, 24.4. Analysis calculated for $C_{15}H_{25}BF_4N_2$: C, 56.27; H, 7.87; N, 8.75. Found: C, 56.56; H, 7.67; N, 8.68.

1,3-Bis(cycloheptyl)imidazolium Bromide (***3***). With the use of cycloheptylamine (2 × 110.4 mmol, Alfa-Aesar, 97%), the procedure for **1** was followed yielding 23.60 g of white solid after drying under high vacuum (69.1 mmol, 63% yield). ^{1}H NMR (300 MHz, DMSO-d_6): 9.44, 7.93, 4.50, 2.08−1.97, 1.95−1.97, 1.77−1.69, 1.65−1.56, 1.54−1.46. ^{13}C NMR (75 MHz, DMSO-d_6): 133.5, 120.8, 61.1, 34.7, 26.8, 23.3. Analysis calculated for $C_{17}H_{29}BrN_2$: C, 59.82; H, 8.56; N, 8.21. Found: C, 59.45; H, 8.33; N, 8.08.

Inorganic Reactions. All inorganic reactions were performed in 23 or 45 mL of poly(tetrafluoroethylene) (PTFE)-lined stainless steel autoclaves (Parr Instruments). Hydroxide mediated reactions were tumbled at approximately 40 rpm using spits built into convection ovens. Fluoride mediated reactions were not tumbled. Silica sources were tetraethylorthosilicate (TEOS, Sigma-Aldrich, 98%) for fluoride reactions and Cab-O-Sil M5 fumed silica (Cabot, 97% SiO_2 with remainder H_2O) for hydroxide mediated reactions. Boric acid (J.T. Baker, ACS Reagent) was used for borosilicate reactions, and Reheis F-2000 (50−53 wt % Al_2O_3) or NaY zeolite (Tosoh HSZ-320NAA, SiO_2/Al_2O_3 = 5.5, Na/Al = 1, and H_2O ∼ 25 wt %) were used in aluminosilicate reactions.

Gels for fluoride mediated reactions were prepared by adding boric acid or aluminum hydroxide gel (if required) to the SDA^+OH^- solution and then adding TEOS. All fluoride mediated reactions were performed at SDA^+OH^-/SiO_2 = 0.5 and HF/SDA^+OH^- = 1. The vessel was covered and stirred overnight to ensure complete TEOS hydrolysis and then left uncovered in a 40 °C oven to evaporate the required water and ethanol. Once the desired mass had been reached, 48 wt % hydrofluoric acid (Mallinckrodt) was added with care and the gel was stirred to form a stiff paste. The autoclave was sealed and placed in a 150 °C oven and opened every 7−10 days to assess reaction progress. After homogenization, a small sample was dispersed in 10 mL of water and inspected under an optical microscope. For certain reactions, small crystals were often visible. If no clear sign of crystallinity could be seen by an optical microscope, a small sample was filtered periodically and the XRD pattern inspected (Scintag XDS-2000 or Siemens D-500, Cu Kα radiation).

Gels for hydroxide mediated reactions were prepared by adding water and 1 N sodium hydroxide solution (if required) to the SDA^+OH^- solution. Next, a boron or aluminum source and then silica were added, followed by homogenization. Borosilicate reactions were run at SiO_2/B_2O_3 = 8 with no alkali hydroxide (gel composition 1.0 SiO_2:0.125 B_2O_3:0.25 SDA^+OH^-:23 H_2O). Aluminosilicate reactions with NaY at a molar silica to alumina (SAR) ratio = 35 had a gel composition of 1.0 SiO_2:0.029 Al_2O_3:0.20 SDA^+OH^-:0.05 NaOH:30.0 H_2O. The remaining reactions used Reheis F-2000 aluminum hydroxide gel as the aluminum source with a gel composition of 1.0 SiO_2:z Al_2O_3:0.20 SDA^+OH^-:0.10 NaOH:30.0 H_2O with z = 0.02 or 0.01.

The inorganic reactions were monitored every 4−6 days by measuring solution pH and looking for signs of phase separation. The reactions were checked until a pH maximum was observed and then filtered. If no pH maximum was observed, the

reaction was continued until a sustained pH decline was observed (indicating SDA degradation). All crude products were washed with water plus a small amount of acetone and methanol and then dried at room temperature. *N*,*N*-dimethylformamide (DMF) extractions were performed on as-made Al-SSZ-70 using ~0.4 g of zeolite and 10 mL of DMF. Solutions were sealed inside PTFE lined autoclaves and heated at 150 °C for 24 h. The extracted product was filtered and washed extensively with water and then dried at room temperature.

Characterization Methods

Powder X-ray diffraction (XRD) patterns were collected using Scintag XDS-2000 and Siemens D-500 diffractometers (Cu Kα radiation). Thermogravimetric analysis (TGA) was performed with a Netzsch STA449C using 75 mL min^{-1} air plus 25 mL min^{-1} argon at a heating rate of 5 °C min^{-1}. Solid-state NMR spectra were collected using either a Bruker Avance 200 MHz or Bruker DSX 500 MHz instrument. ^{29}Si Bloch decay (BD) experiments on as-made materials used a 500 s recycle delay. ITQ-1 (MWW) ^{29}Si chemical shift data was obtained from published studies.[5] Scanning electron microscopy (SEM) was performed using a JEOL JSM-6700F instrument. Elemental analyses were performed by Galbraith Laboratories (Knoxville, TN).

Nitrogen adsorption/desorption isotherms were collected on a Micromeritics ASAP 2000 instrument at −196 °C. Micropore volumes were calculated using the t-plot method. The adsorption capacities of zeolites for vapor phase hydrocarbons *n*-hexane, 3-methylpentane, and 2,2-dimethylbutane were measured at room temperature using a Cahn C-2000 balance coupled with a Yokogawa digital data acquisition system.[6,7] The vapor of the adsorbate was delivered from the liquid phase with a 99.5+% purity guaranteed by the manufacturer (Sigma-Aldrich). The relative vapor pressure *P*/Po was maintained at ~0.3 by controlling the temperature of the liquid adsorbate using a cooling circulator. Prior to the adsorption experiments, the calcined zeolites were degassed at 450 K in a vacuum of 10^{-3} Torr for 5 h. The sample size was controlled at ~20 mg of dry zeolite for all experiments. The adsorption capacities are reported in milliliters of liquid per gram of dry zeolite, assuming that the adsorbed adsorbate has the same density as the bulk liquid (e.g., 0.660 g mL^{-1} for *n*-hexane, 0.663 g mL^{-1} for 3-methylpentane, and 0.649 g mL^{-1} for 2,2-dimethylbutane at room temperature).

Catalytic Testing. Catalytic activity of Al-SSZ-70 materials was evaluated through the constraint index test.[4] As-made Al-SSZ-70 synthesized using NaY as the aluminum source was treated with 1 N HCl at 95 °C for 48 h to neutralize any residual NaY that may affect catalytic activity.[8]

(5) Camblor, M. A.; Corma, A.; Diaz-Cabanas, M. J.; Baerlocher, C. *J. Phys. Chem. B* **1998**, *102*(1), 44–51.
(6) Chen, C. Y.; Zones, S. I. *Microporous Mesoporous Mater.* **2007**, *104* (1−3), 39–45.
(7) Zones, S. I.; Chen, C. Y.; Corma, A.; Cheng, M. T.; Kibby, C. L.; Chan, I. Y.; Burton, A. W. *J. Catal.* **2007**, *250*(1), 41–54.
(8) Zones, S. I.; Nakagawa, Y.; Lee, G. S.; Chen, C. Y.; Yuen, L. T. *Microporous Mesoporous Mater.* **1998**, *21*(4−6), 199–211.

Table 1. Fluoride Reaction Conditions for the Synthesis of SSZ-70

entry	SDA	$SiO_2/(Al_2O_3,B_2O_3)$	H_2O/SiO_2	result
1	**1**	∞	3.5	Si-SSZ-70
2	**1**	∞	7.5	Si-SSZ-70
3	**1**	∞	14.5	MTW
4	**1**	30	15.5	Al-SSZ-70
5	**1**	50	15.5	Al-SSZ-70
6	**1**	70	15.5	Al-SSZ-70[a]
7	**1**	11	15.5	B-SSZ-70
8	**1**	36	15.5	B-SSZ-70
9	**3**	∞	14.5	Si-SSZ-70

[a] Minor impurity present.

The SDA occluded within as-made SSZ-70 was expected to protect the framework aluminum with only unreacted NaY affected by the HCl treatment. The sample of SSZ-25 used in this study came from a 5 gallon preparation of the material using a mixed SDA system of *N*,*N*,*N*-2-trimethyladamantammonium hydroxide and piperidine as a pore filler as previously described.[9] All SSZ-70 materials were calcined to 540 °C at a heating rate of 1 °C min^{-1} under flowing nitrogen with a small amount of air. Calcined materials were ion-exchanged with 1 N NH_4NO_3 at 50 °C and then filtered and washed with distilled deionized water. The ammonium-exchanged materials were pelletized, crushed, and sieved with the 20−40 mesh fraction collected. Sized material (typically 0.5 g) was loaded into a stainless steel tube reactor supported by glass wool and activated by heating under flowing argon at 350 °C for at least 4 h. Reactions were performed at 350 °C unless otherwise noted. Hydrocarbon cracking in the CI tests was performed by introducing an equimolar *n*-hexane/3-methylpentane mixture (both from Sigma-Aldrich, ≥99.9%) via a syringe pump into a mixing assembly with 5% argon in helium sweep gas (Airliquide, 99.999%) (LHSV = 1.67 h^{-1}). Products were analyzed using online gas chromatography/mass spectrometry (GC/MS; Agilent GC 6890/MSD 5973N) with a Plot-Q capillary column.

Results and Discussion

Tables 1 and 2 present the conditions used for synthesizing SSZ-70 in this work. When possible, characterization was performed on SSZ-70 materials synthesized using the same SDA. Most reactions employed bis(isobutyl) SDA **1**, as this molecule was capable of synthesizing pure silica, borosilicate, and aluminosilicate SSZ-70. The pure silica fluoride reaction using **1** at a high water to silica ratio was also included for chemical analysis comparison. SDA **1** did not make pure Si-SSZ-70 under hydroxide mediated reaction conditions; therefore, Si-SSZ-70(OH) using bis(cyclohexyl) SDA **2** or bis(cycloheptyl) SDA **3** were employed. Products were denoted with (OH) or (F) to indicate the appropriate synthesis conditions. Nitrogen adsorption experiments were conducted with Si-SSZ-70(OH) synthesized using SDA **2** while ^{29}Si NMR analyses were with Si-SSZ-70 (F)

(9) Zones, S. I.; Hwang, S. J.; Davis, M. E. *Chem.—Eur. J.* **2001**, *7*(9), 1990–2001.

Table 2. Hydroxide Mediated Reaction Conditions for the Synthesis of SSZ-70

entry	SDA	$SiO_2/(Al_2O_3,B_2O_3)$	result
1	**1**	50	Al-SSZ-70
2	**1**	100	Al-SSZ-70
3	**1**	8	B-SSZ-70
4	**2**	35	Al-SSZ-70
5	**2**	∞	Si-SSZ-70
6	**3**	∞	Si-SSZ-70

and Si-SSZ-70 (OH) synthesized using SDA **3**. Hydrocarbon adsorption was performed with Al-SSZ-70(F) synthesized using SDA **1** (entry 5 in Table 1).

Powder XRD patterns are shown in Figures 1−3 for as-made and calcined SSZ-70. Inspection of the powder XRD pattern reveals similarity to those obtained from MWW precursor materials. Figure 1 shows XRD patterns for as-made Al-SSZ-70 synthesized in fluoride and hydroxide media using **1** (Al-SSZ-70(F) and Al-SSZ-70-(OH), respectively). Also included in Figure 1 is the XRD pattern of as-made SSZ-25 as a representative MWW material. All three materials give quite sharp reflections at 26.0° 2θ, indicating similar structural features may be present in both materials. While some similarities were apparent between MWW and SSZ-70 from the XRD patterns (as illustrated in Figure 1), there were no instances of MWW from any of the many syntheses performed with the 16 imidazolium SDAs studied across 160 inorganic reactions.[2] Figure 2 is an enlargement of the XRD patterns illustrated in Figure 1 in the 2−12° 2θ range. The pattern for the as-made product shows one reflection with large *d*-spacing (3.22° 2θ, 27.4 Å), and several integer divisors are also present. The pattern for Al-SSZ-70(OH) is considerably broader than both SSZ-25 and Al-SSZ-70(F) with the low angle reflection appearing as a weak shoulder. Broad reflections in the hydroxide material were likely due to smaller crystal size (from SEM results). Inspection of the low-angle features in Figure 2 reveals higher *d*-spacings for SSZ-70 compared to MWW materials. Higher *d*-spacings in this region of the XRD patterns compared to MWW were also reported for ITQ-30.[10] Comparing the patterns for hydroxide- and fluoride-mediated products reveals the same *d*-spacing for all reflections except one broad reflection at 8.7° 2θ for the fluoride product whereas the hydroxide product gives two reflections at 7.9 and 9.5° 2θ. This diffraction intensity difference could be due to differences in crystal size along the *c*-direction (orthogonal to layers) as observed in DIFFaX simulations of MCM-22 and MCM-56.[11]

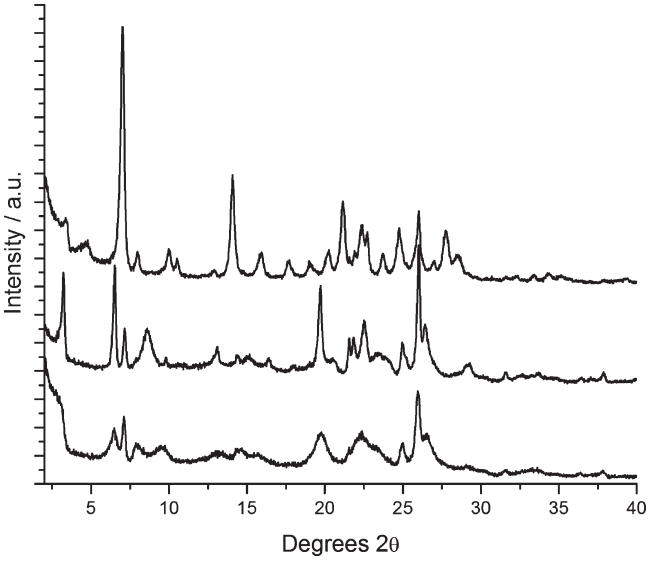

Figure 1. XRD patterns of as-made SSZ-25 (top), Al-SSZ-70(F) (middle), and Al-SSZ-70(OH) (bottom).

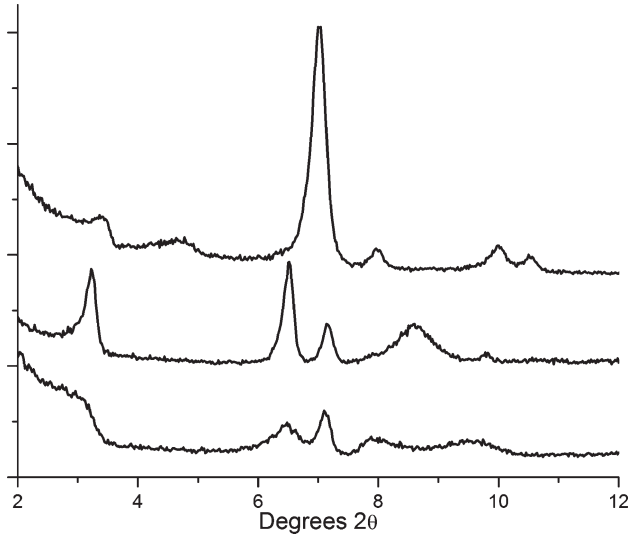

Figure 2. XRD patterns of as-made SSZ-25 (top), Al-SSZ-70(F) (middle), and Al-SSZ-70(OH) (bottom).

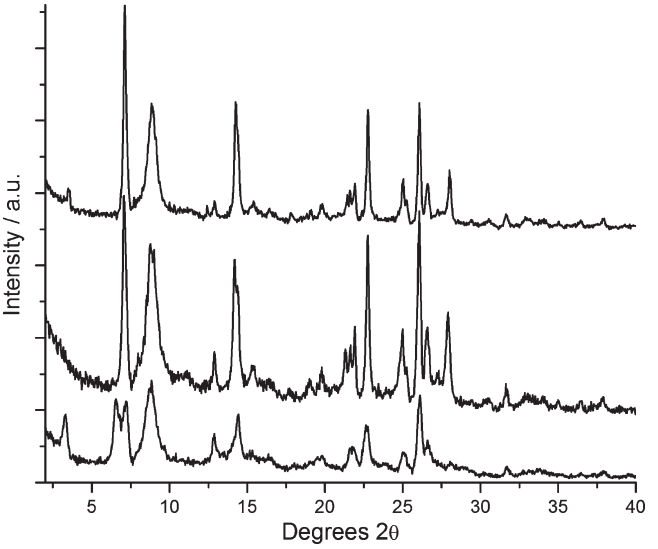

Figure 3. XRD patterns of calcined Si-SSZ-70(F) (top), Al-SSZ-70(F) (middle), and B-SSZ-70(F) (bottom).

Figure 3 shows XRD patterns for calcined SSZ-70 materials synthesized in fluoride media using **1**. Shown are pure silica (Si-SSZ-70(F)), borosilicate (B-SSZ-70(F)) ,and aluminosilicate (Al-SSZ-70(F)) materials. For both

(10) Corma, A.; Diaz-Cabanas, M. J.; Moliner, M.; Martinez, C. *J. Catal.* **2006**, *241*(2), 312–318.
(11) Juttu, G. G.; Lobo, R. F. *Microporous Mesoporous Mater.* **2000**, *40* (1−3), 9–23.

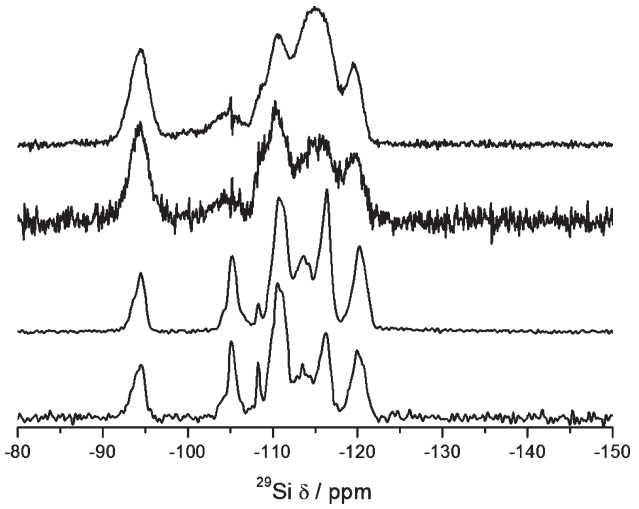

Figure 4. Solid-state ^{29}Si NMR spectra of Si-SSZ-70. Top to bottom: Si-SSZ-70(OH) CP-MAS, Si-SSZ-70(OH) BD-MAS, Si-SSZ-70(F) CP-MAS, and Si-SSZ-70(F) BD-MAS.

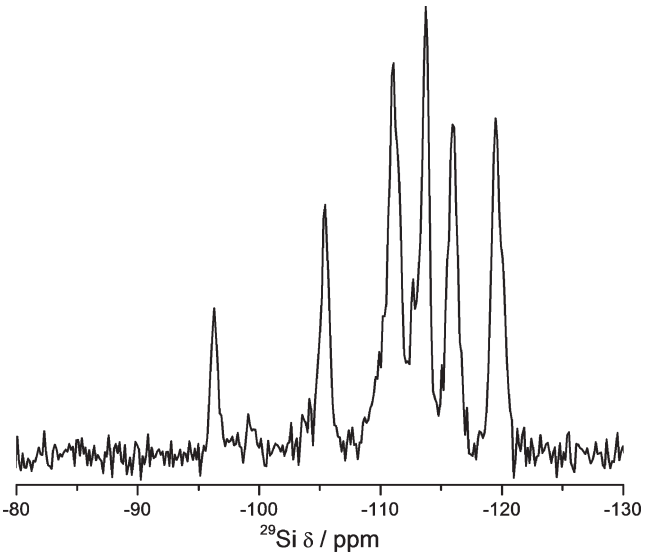

Figure 5. Solid-state ^{29}Si BD-MAS NMR of calcined Si-SSZ-70(F).

Si-SSZ-70(F) and Al-SSZ-70(F), the two low-angle reflections present in the as-made material (3.2 and 6.5° 2θ) were absent or appear with reduced intensity after calcination. The first significant reflection occurs at 7.0° 2θ (~12.5 Å) in both materials. In contrast, the low-angle reflections (3.2 and 6.5° 2θ) persist after calcination for B-SSZ-70(F) albeit with lower relative intensity. Both low-angle reflections were not observed after calcining B-SSZ-70(OH).

Solid-state ^{29}Si NMR was performed on Si-SSZ-70(F) and Si-SSZ-70(OH). Spectra were collected on samples obtained using bis(cycloheptyl) SDA **3**. Figure 4 shows ^{1}H−^{29}Si cross-polarization magic angle spinning (CP MAS) and ^{29}Si Bloch decay (BD MAS) spectra of as-made Si-SSZ-70 samples. Both spectra for as-made solids show significant Q^3 silicon content (−94 ppm resonance). A comparison of the CP and BD spectra reveal a higher relative intensity for the −116 and −120 ppm resonances under CP conditions (2 ms contact time) and a relative decrease for the −108 ppm resonance. The resonances in the fluoride-mediated sample are well-defined and span a similar chemical shift range to those reported for ITQ-1.[5,12] The spectrum of calcined Si-SSZ-70(F) illustrated in Figure 5 shows six well resolved resonances with a small amount of Q^3 silicon still present.

Table 3 lists the observed chemical shifts for as-made Si-SSZ-70 materials. Relative intensity was determined by integration of the BD MAS spectra. In general the resonances for Si-SSZ-70 samples are not as well resolved as those for ITQ-1. This was particularly true for the hydroxide mediated sample. No attempt was made to deconvolute the spectra as the limited resolution did not warrant this. Therefore, fewer chemical shifts are included in the table. Inspecting the relative intensities shows a significant population of Q^3 silica species in both hydroxide- and fluoride-mediated samples. The

Table 3. ^{29}Si Chemical Shifts and Relative Intensities for As-Made Si-SSZ-70(OH), Si-SSZ-70(F), and ITQ-1

Si-SSZ-70 (OH)		Si-SSZ-70 (F)		ITQ-1		
δ/ppm	I/%	δ/ppm	I/%	δ/ppm	assignment	I/%
				−92.6	Q^3	12.0
−94.1	22.1	−94.6	10.5	−94.1	Q^3	19.0
−104.3	6.4	−105.2	11.5	−103.7	Q^3	1.9
−110.4	30.1	−108.3	4.9	−105.0	Q^4	2.8
−115.6	27.9	−110.6	30.5	−108.3	Q^4	1.7
−119.7	13.5	−113.5	12.1	−110.1	Q^4	27.8
		−116.3	15.6	−112.4	Q^4	2.5
		−119.9	14.8	−114.7	Q^4	10.7
				−116.7	Q^4	10.1
				−119.8	Q^4	11.5

Table 4. ^{29}Si Chemical Shifts and Relative Intensities for Calcined Si-SSZ-70(F) and ITQ-1

Si-SSZ-70(F)		ITQ-1		
δ/ppm	I/%	δ/ppm	assignment	I/%
−96.3	4.6			
−105.4	11.5	−105.9	Q4	15.1
−111.0	25.9	−111.2	Q4	15.1
−113.7	23.1	−111.8	Q4	4.9
−116.0	17.3	−112.6	Q4	7.6
−119.5	17.6	−113.9	Q4	19.0
		−116.5	Q4	18.9
		−120.3	Q4	19.4

resonance < −100 ppm for each sample can be assigned as Q^3, but there was some ambiguity regarding the resonances near −105 ppm. The spectrum for calcined Si-SSZ-70(F) illustrated in Figure 5 clearly shows the −105 ppm resonance, whereas the −95 ppm resonance is significantly diminished. This result suggests the −105 ppm resonance to be Q^4 in order to give a relative Q^3 abundance of ~10% in the as-made material. The broad resonance centered at −104 ppm for the hydroxide mediated material could not be conclusively assigned to either Q^3 or Q^4 giving an estimated relative Q^3 population of ~22−28%. The upper estimate for Q^3 content in the hydroxide mediated sample is in general agreement with those reported for ITQ-1 (29−33%). For as-made

(12) Camblor, M. A.; Corell, C.; Corma, A.; Diaz-Cabanas, M.-J.; Nicolopoulos, S.; Gonzalez-Calbet, J. M.; Vallet-Regi, M. *Chem. Mater.* **1996**, *8*(10), 2415–2417.

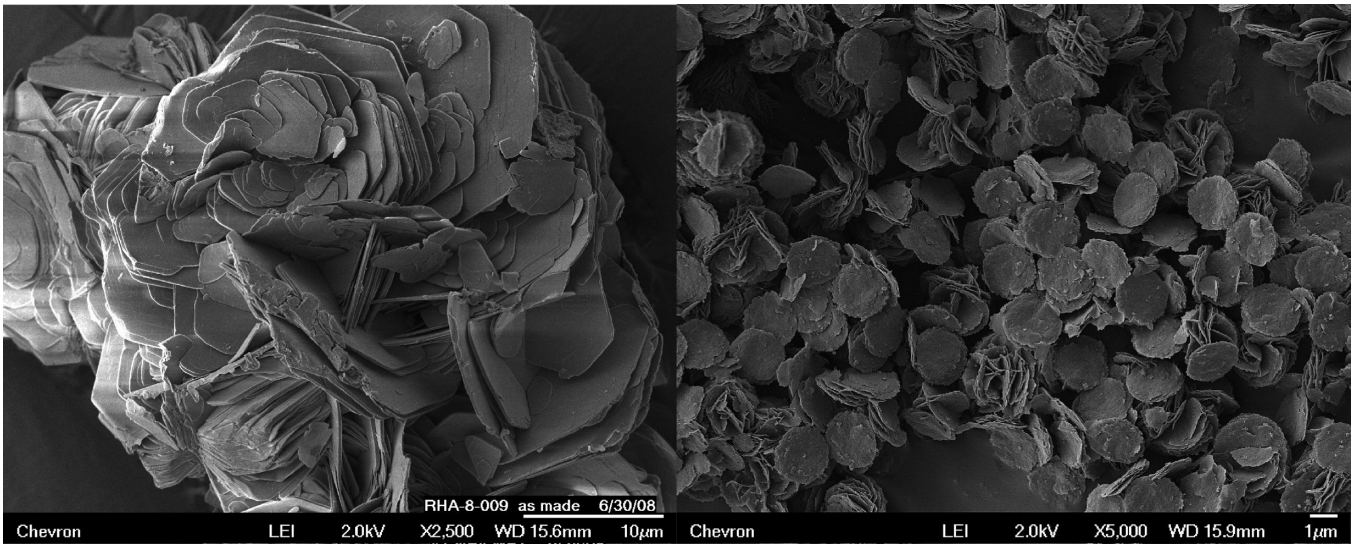

Figure 6. SEM images of as-made Si-SSZ-70(F) (left) and calcined Al-SSZ-70(OH) (right). The scale bar represents 10 and 1 μm for the left and right images, respectively.

Si-SSZ-70(F), there was no analogous material to compare the relative Q^3 population as fluoride reactions generally produce solids with very few defects (low Q^3). In addition, no evidence of $SiO_{4/2}F$ species was observed between −130 and −150 ppm in as-made Si-SSZ-70(F). Chemical analysis did show fluorine incorporation as discussed below. The exact nature of the fluoride species present in Si-SSZ-70 is not understood, although a report of MWW synthesis with alkali fluoride salts proposed $SiO_{3/2}F$ may be present.[13] With this interpretation, fluorine may substitute for surface hydroxyl groups and therefore skew the relative Q^3/Q^4 ratio. It should be noted that ^{19}F MAS NMR revealed one dominant resonance at −69 ppm (data not shown) with this in the expected range for $SiO_{4/2}F$.[14]

The chemical shifts and relative intensities for calcined Si-SSZ-70(F) presented in Table 4 show several differences. As mentioned above, calcination did not completely remove all Q^3 species. In addition, the resonance of the as-made product at −108.3 ppm is not visible in the spectrum of the calcined product. These observations plus the fact that the relative decrease in intensity in the $^1H-^{29}Si$ spectrum may indicate the presence of $SiO_{3/2}F$ species. The observed chemical shifts and relative intensities show similarity to those of ITQ-1.

SEM images of Si-SSZ-70(F) and Al-SSZ-70(OH) are shown in Figure 6. Thin hexagonal plates were visible in the fluoride-mediated reaction product. In comparison, the hydroxide-mediated product revealed significantly smaller crystallites. MWW materials form crystals with similar morphology. The observed crystal morphology supports the similarity to MWW materials (similarities also observed by XRD and ^{29}Si NMR). Figure 7 shows a transmission electron microscopy (TEM) image of B-SSZ-70 with a view through the edges of the crystal plates. Note that the layers are clearly observed. Images at higher magnification did not show pore features as observed for MCM-22[15] and SSZ-25.[16]

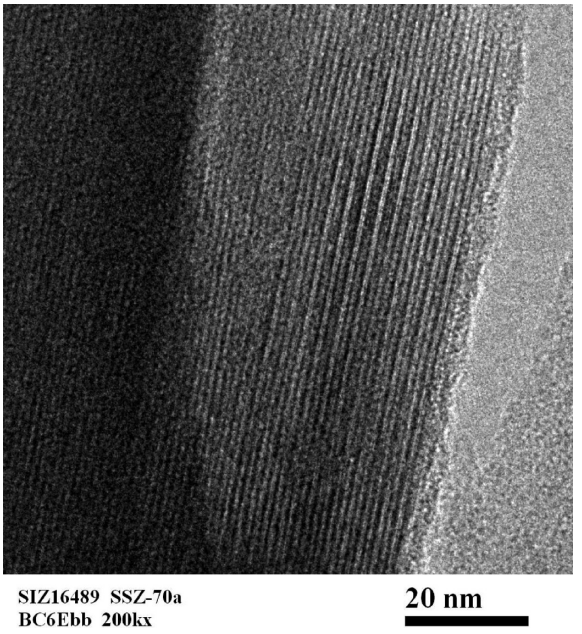

Figure 7. TEM image of B-SSZ-70.

Table 5. Carbon, Nitrogen, and Fluorine Content for Pure-Silica Products from Fluoride Mediated Reactions Using SDA 1

	H_2O/SiO_2 = 3.5 (SSZ-70)	H_2O/SiO_2 = 7.5 (SSZ-70)	H_2O/SiO_2 = 14.5 (MTW)
C/wt %	11.91	13.65	6.94
N/wt %	2.41	2.79	1.43
F/w t%	0.69	0.83	1.06
C/N	5.76	5.71	5.66
F/N	0.21	0.22	0.55

(13) Aiello, R.; Crea, F.; Testa, F.; Demortier, G.; Lentz, P.; Wiame, M.; Nagy, J. B. *Microporous Mesoporous Mater.* **2000**, *35*−*6*, 585–595.
(14) Koller, H.; Wolker, A.; Villaescusa, L. A.; Diaz-Cabanas, M. J.; Valencia, S.; Camblor, M. A. *J. Am. Chem. Soc.* **1999**, *121*(14), 3368–3376.
(15) Leonowicz, M. E.; Lawton, J. A.; Lawton, S. L.; Rubin, M. K. *Science* **1994**, *264*(5167), 1910–1913.
(16) Chan, I. Y.; Labun, P. A.; Pan, M.; Zones, S. I. *Microporous Mater.* **1995**, *3*(4−5), 409–418.

Table 6. Chemical Analysis of B-SSZ-70(F), Al-SSZ-70(F), and Al-SSZ-70(OH)

	gel composition ratio						
	Si/B = 18	Si/B = 5.5	Si/Al = 35	Si/Al = 25	Si/Al = 15	Si/Al = 50	Si/Al = 25
C/wt %	13.67	13.51	12.23	13.07	13.54	13.62	13.37
N/wt %	2.80	2.77	2.57	2.71	2.70	2.82	2.81
F/wt %	1.16	1.04	0.70	0.64	0.82		
C/N	5.7	5.7	5.6	5.6	5.8	5.6	5.6
F/N	0.31	0.28	0.20	0.18	0.22		
Na/wt %						0.17	0.14
Si/B	21.7	13.7					
Si/Al			34.1	25.5	16.6	44.4	22.2

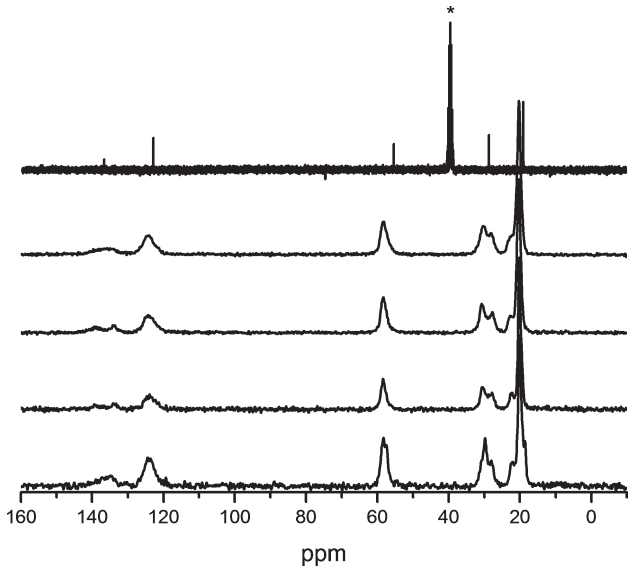

Figure 8. ^{13}C CP-MAS of SSZ-70 solids synthesized using SDA **1**. Top to bottom = parent SDA in DMSO-d_6 (∗ indicates solvent), B-SSZ-70(OH), B-SSZ-70(F), Al-SSZ-70(F), and Al-SSZ-70(OH).

Chemical analyses were performed on SSZ-70 materials to gain further insights. All samples were synthesized using bis(isobutyl) SDA **1**. Also included was pure-silica MTW synthesized at H_2O/SiO_2 = 14.5, representing typical fluoride mediated reaction products. Table 5 presents chemical analysis data for pure-silica products from fluoride mediated reactions, and Table 6 contains chemical analysis for B-SSZ-70 and Al-SSZ-70 materials. Calculated carbon to nitrogen molar ratios agree with those expected for the parent SDA. In addition, both imidazolium (135−120 ppm) and alkyl resonances (60−20 ppm) were observed by ^{13}C CP-MAS NMR in SSZ-70 solids (Figure 8). These results confirm that the SDA was intact.

The calculated fluoride to nitrogen molar ratios are shown in Tables 5 and 6, and all F/N ratios can be compared to the theoretical F/N value for the SDA^+F^- salt (0.50 for all imidazolium SDAs studied). This value corresponds to a neutral product with no framework defects to balance the charge of the organic cation. MTW synthesized using **1** gave F/N = 0.55 that was very close to the expected value for no framework defects. By comparison, the two Si-SSZ-70 products show significantly lower F/N ratios and this extends to the boron and aluminum containing materials. Fluoride absence implies that the organic charge must be balanced by silanol defects as observed by ^{29}Si NMR above.[17]

Chemical analysis of B-SSZ-70(F), Al-SSZ-70(F), and Al-SSZ-70(OH) in Table 6 shows very similar organic content across the seven products. Carbon to nitrogen molar ratios are between 5.6 and 5.8 agreeing well with the expected ratio of 5.5. Slightly higher fluorine content was measured in the borosilicate samples compared to the pure-silica and aluminosilicate samples. With trivalent lattice substitution (B or Al), a framework charge is introduced and fluoride is no longer required to balance the cation charge. However, the calculated F/N ratios show little variation with lattice substitution for both boron and aluminum incorporation, respectively. In addition, the F/N ratios for all three aluminosilicate samples are almost the same as the pure silica products. The report of MCM-22 synthesis using hexamethyleneimine with alkali fluoride salts discussed above showed varying amounts of fluoride incorporated in the aluminosilicate product.[13] Under the approximately neutral reaction conditions the secondary amine should be protonated and similar cation/framework charge arguments must hold.

Inspection of the Si/B and Si/Al ratios measured in the as-made products reveals less boron incorporation than is present in the reaction gel. By comparison, aluminosilicate products synthesized via both fluoride and hydroxide conditions reveal Si/Al ratios almost identical to those in the reaction gel. These data agree with reported trends in boron and aluminum incorporation for products from hydroxide reactions using the same SDA.[18] Chemical analysis for both hydroxide mediated products shows some sodium incorporation. The measured Na/Al values correspond to ~0.25 and 0.11 for Si/Al = 50 and Si/Al = 25, respectively, indicating the framework charge was predominantly compensated by SDA rather than alkali. This suggests organic occupies most of the void space within SSZ-70 in contrast to SSZ-25 where the bulky adamantyl SDA was not expected to fit in the sinusoidal 10MR.[9]

In addition to chemical analysis, TGA was performed on SSZ-70 products. Figure 9 compares the TG profiles for Si-SSZ-70(F) synthesized using **1** and **2**. Both materials show very similar mass loss between 200 and 620 °C (19.3% for **1** and 20.4% for **2**), yet the mass loss profiles are distinct. The smaller bis(isobutyl) SDA **1** shows one

(17) Koller, H.; Lobo, R. F.; Burkett, S. L.; Davis, M. E. *J. Phys. Chem.* **1995**, *99*(33), 12588–12596.

(18) Zones, S. I.; Hwang, S.-J. *Microporous Mesoporous Mater.* **2003**, *58* (3), 263–277.

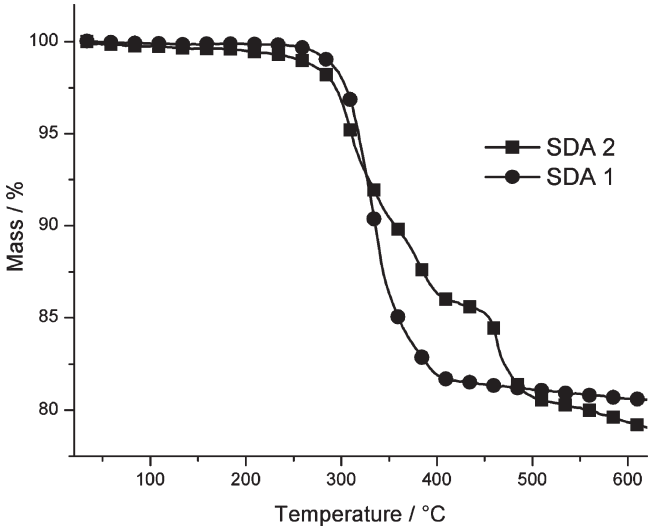

Figure 9. TGA of as-made Si-SSZ-70(F) synthesized using SDA **1** and SDA **2**.

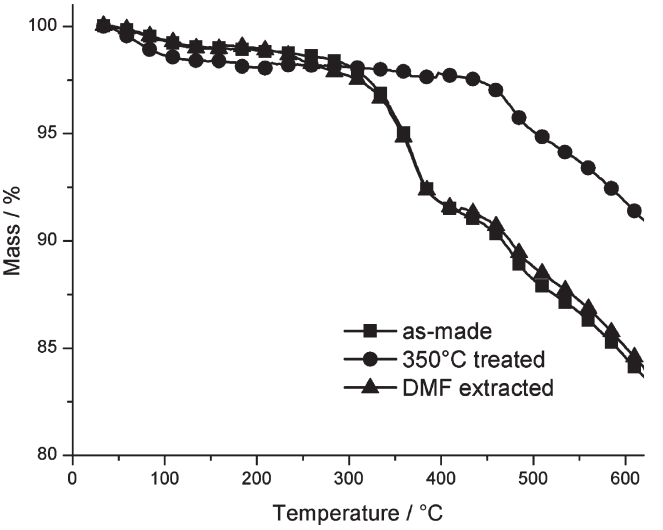

Figure 10. TGA of Al-SSZ-70(OH) synthesized using SDA **2** before and after postsynthetic treatments.

mass loss starting at approximately 250 °C, whereas two mass loss regions can be seen for the larger bis(cyclohexyl) SDA **2**. The first mass loss starts at around 250 °C as per **1** with an inflection point at ~425 °C followed by another mass loss. Observing two mass loss regions with the larger SDA could indicate two distinct organic environments. With as-synthesized SSZ-70 most likely being a layered material, the first mass loss can be assigned to organic occluded between layers and the second mass loss attributed to organic occluded within the layers. Observing one mass loss with the smaller SDA was likely due to a weaker fit within the framework offering lower thermal protection.

Several postsynthesis experiments were performed on an Al-SSZ-70 sample synthesized using **2** to gain insight into the relative contribution of each organic environment. The sample was obtained from reaction conditions that use the SAR = 35 NaY as an aluminum source, and the product treated with 1 N HCl to neutralize residual FAU species as described in the Experimental Section. The first experiment explored SDA removal by DMF extraction. Similar experiments with SSZ-25 showed organic removal and significant changes in the XRD pattern after DMF extraction.[9] No organic removal was detected by TGA after extraction for the Al-SSZ-70 material studied. In addition, the XRD pattern was identical to the parent material. The inability to remove organic by DMF extraction suggests an organic/framework environment similar to traditional zeolites where extraction does not typically remove organic. The second experiment thermally treated the as-made Al-SSZ-70 material to remove the organic species associated with the lower temperature weight loss region (Figure 10). Inspecting the TGA profiles indicated 350 °C was sufficient to remove organic residing in the first environment, and 350 °C should be approximately 75 °C below the mass loss onset of the second environment. After the sample was heated at 350 °C for 5 h in air, all organic below 425 °C was removed and the XRD pattern showed clear

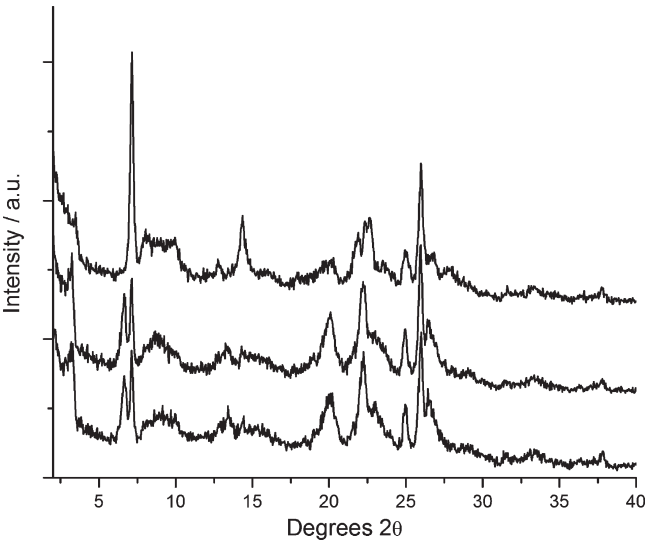

Figure 11. XRD patterns of Al-SSZ-70(OH) synthesized using **2** before and after postsynthetic treatments. From bottom to top: parent material, DMF extracted, and 350 °C treated.

differences. TGA profiles and XRD patterns of the samples after DMF extraction and thermal treatment are shown in Figures 10 and 11, respectively. The XRD pattern resembled calcined Al-SSZ-70(OH) even though ~7 wt % organic remained occluded. This heat treated material was ammonium-exchanged and assessed for micropore volume and catalytic activity as described below.

Micropore volumes of SSZ-70 products were obtained using nitrogen adsorption. All SSZ-70 samples examined were synthesized using **1** except Si-SSZ-70(OH) that used **2** and the Al-SSZ-70(OH) 350 °C treated sample synthesized using **2**. Table 7 lists micropore volume for each SSZ-70 material. These data show a clear distinction between the fluoride and hydroxide mediated products with a 0.20 $cm^3\ g^{-1}$ micropore volume observed from all three fluoride mediated products and 0.09−0.14 $cm^3\ g^{-1}$ obtained from the hydroxide mediated products. The

Table 7. Micropore Volumes of SSZ-70 Products

SSZ-70 product	micropore volume /cm^3 g^{-1}
Si-SSZ-70 (F)	0.20
B-SSZ-70 (F)	0.20
Al-SSZ-70 (F)	0.20
Si-SSZ-70 (OH)	0.09
B-SSZ-70 (OH)	0.12
Al-SSZ-70 (OH)	0.14
Al-SSZ-70 (OH) treated at 350 °C	0.09

micropore volumes for the fluoride products are similar to those reported for MWW materials (0.17−0.18 cm^3 g^{-1}).[12] The 350 °C treated material shows approximately two-thirds the micropore volume of calcined Al-SSZ-70(OH) material. Assuming this organic resides in interlayer regions, this gives a similar contribution as reported for SSZ-25 where ~0.12 cm^3 g^{-1} micropore volume was attributed to the large cages formed between layers.

Hydrocarbon adsorption was performed to gain insight into possible pore sizes. Figure 12 shows the time dependence of the adsorption capacity of *n*-hexane, 3-methylpentane, and 2,2-dimethylbutane in SSZ-70 and SSZ-25. The kinetic diameters of these three molecules are 4.4 Å for *n*-hexane, 5.0 Å for 3-methylpentane, and 6.2 Å for 2,2-dimethylbutane. The fast uptakes of *n*-hexane and 3-methylpentane (both are the reactants for the constraint index test to be discussed below) in both SSZ-70 and SSZ-25 indicate that the diffusion of the molecules of these two adsorbates is not hindered in channel systems of these two zeolites. These results also imply that the catalytic cracking reactions of *n*-hexane and 3-methylpentane occurring in the constraint index test of SSZ-70 and SSZ-25 are not controlled by the reactant shape selectivity. The slow uptakes of 2,2-dimethylbutane observed in both SSZ-70 and SSZ-25 indicate that the effective size of the pore openings of SSZ-70 and SSZ-25 become especially critical to the diffusivity of bulkier 2,2-dimethylbutane molecules, as previously reported for 10-ring zeolites.[6,7] Therefore, these results suggest that SSZ-70 is a medium pore zeolite.

Catalytic Activity. The constraint index test is used here as a model acid-catalyzed hydrocarbon reaction. Four

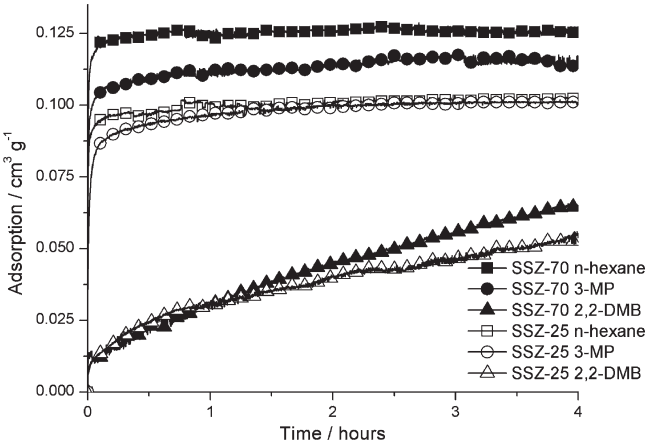

Figure 12. Hydrocarbon adsorption vs time for SSZ-70 and SSZ-25. 3-MP is 3-methylpentane, and 2,2-DMB is 2,2-dimethylbutane.

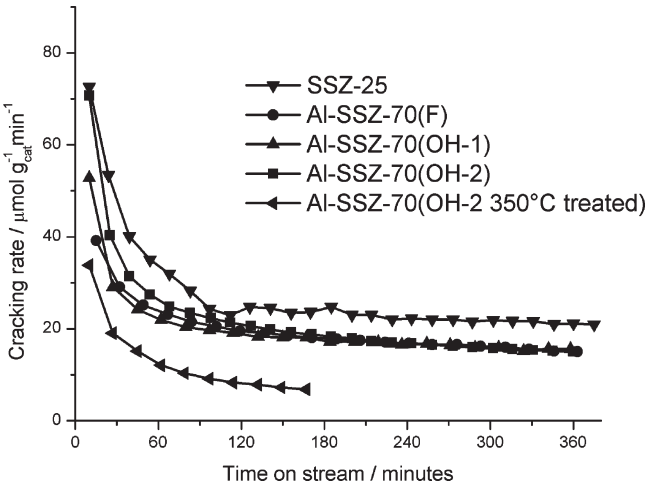

Figure 13. CI test cracking rate vs time on stream for Al-SSZ-70 materials: Al-SSZ-70(OH-**1**)=Al-SSZ-70(OH) synthesized using SDA **1** and Al-SSZ-70(OH-**2**)=Al-SSZ-70(OH) synthesized using SDA **2**.

Al-SSZ-70 materials were tested: Al-SSZ-70(F, Si/Al = 26) and Al-SSZ-70(OH, Si/Al = 22) synthesized using **1** plus Al-SSZ-70(OH) and the 350 °C treated material synthesized using **2**. The physicochemical characterizations outlined above for SSZ-70 showed similarity to MWW materials, so SSZ-25 was included for comparison (the SSZ-25 CI test reaction was performed at 330 °C). Figure 13 shows the cracking rate as a function of time on stream (TOS). Results from a more comprehensive study on the CI test behavior reported high initial activity for SSZ-25 that was comparable to BEA* and greater than MFI, which was followed by rapid deactivation.[19] The three SSZ-70 materials shown here behave similarly. The deactivation with TOS follows a similar path as SSZ-25. The 350 °C treated material shows the same deactivation trend although the initial rate was significantly lower than for all other materials owing to a lower number of active sites. These data suggest a similarity to MWW materials; however, the CI value versus TOS relationships shown in Figure 14 present a clear distinction between SSZ-70 and SSZ-25. All materials reveal initial CI values < 1 with SSZ-25 giving a rapid increase as previously described.[20] By contrast, all SSZ-70 materials maintain CI values < 1.2 throughout the reaction. With regards to the TOS behavior of SSZ-25, it was postulated the deactivation rates of the two independent pore systems were different giving rise to a changing CI value. Both pore systems could contribute to the initial reactivity, with the more accessible MWW cage dominating over the sinusoidal pore system. The high initial activity from active sites located within the cages may mask the sinusoidal pore reactivity. As active sites in the cages deactivated due to fouling, the sinusoidal pores can account for relatively higher reactivity resulting in an increase in the CI value to the range expected for medium pore materials (1 < CI < 12). MWW deactivation in *n*-heptane cracking at 350 °C showed carbonaceous

(19) Carpenter, J. R.; , Yeh, S.; , Zones, S. I.; Davis, M. E. J. Catal. In press.
(20) Zones, S. I.; Harris, T. V. *Microporous Mesoporous Mater.* **2000**, *35−6*, 31–46.

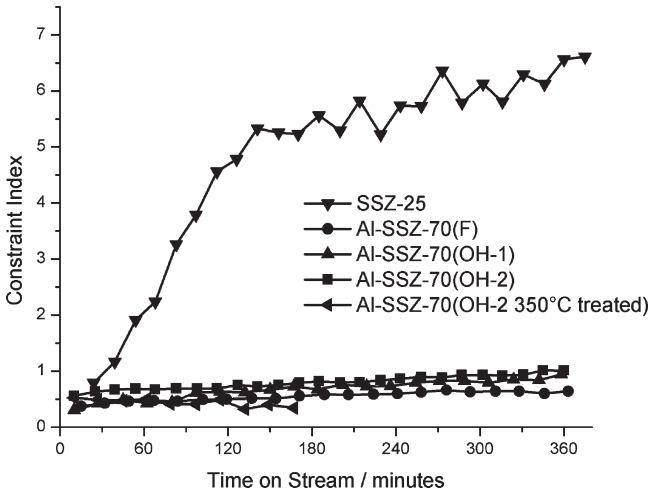

Figure 14. Constraint index vs time on stream for Al-SSZ-70 materials: Al-SSZ-70(OH-**1**)=Al-SSZ-70(OH) synthesized using SDA **1** and Al-SSZ-70(OH-**2**)=Al-SSZ-70(OH) synthesized using SDA **2**.

deposits only formed in supercages with no deactivation observed in the sinusoidal channels.[21] All SSZ-70 materials reveal similar cracking rate deactivation suggesting the presence of a similar cavity, but the absence of an increasing CI value as the material deactivates suggests a second pore system distinct to the sinusoidal 10MR pore found in MWW.

(21) Matias, P.; Lopes, J. M.; Laforge, S.; Magnoux, P.; Guisnet, M.; Ribeiro, F. R. *Appl. Catal., A* **2008**, *351*(2), 174–183.

Conclusions

Pure silica, borosilicate, and aluminosilicate SSZ-70 materials were characterized and showed some similarity to MWW materials. XRD analysis of as-made products indicated that SSZ-70 has slightly larger layer spacing compared to MWW. Si-SSZ-70 showed very similar ^{29}Si MAS NMR resonances to ITQ-1, suggesting SSZ-70 could be a disordered MWW material. All SSZ-70 materials synthesized under fluoride conditions had lower fluorine content than expected for a defect free material. Fluoride absence requires silanol defects to balance organic charge, and this accounted for the Q^3 silicon observed by ^{29}Si MAS NMR. Al-SSZ-70 catalytic behavior was assessed through the CI test with distinct differences observed in CI as a function of TOS compared to SSZ-25 (MWW). Cracking rate as a function of TOS was qualitatively the same between SSZ-70 and SSZ-25, suggesting a similar feature to the large MWW cavity might be present in SSZ-70. The absence of increasing CI with TOS in SSZ-70 materials could indicate a different secondary pore system is present compared to the sinusoidal 10-ring channel in MWW.

Acknowledgment. This work was supported by the Chevron Energy Technology Company. Electron microscopy was performed by I. Y. Chan and Tom Rea (Chevron Energy Technology Company). The NMR facility at Caltech was supported by the National Science Foundation (NSF) under Grant Number 9724240 and partially supported by the MRSEC Program of the NSF under Award Number DMR-0520565.